INHIBITED ALUMINIZATION OF AN ODS FeCr ALLOY – A. Vande Put and B. A. Pint (Oak Ridge National Laboratory, USA)

OBJECTIVE

One proposed U.S. test blanket module (TBM) for ITER uses reduced activation ferritic-martensitic (FM) steels with both eutectic Pb-Li and He coolants at ~475°C. In order for this blanket concept to operate at higher temperatures (~700°C) for a DEMO-type reactor, several Pb-Li compatibility issues need to be addressed. One strategy to reduce dissolution of conventional and dispersion-strengthened FM steels in Pb-Li above 500°C is to aluminize the surface. The performance of coatings is currently being evaluated.

SUMMARY

Prior work characterized the performance of Al-rich coatings made by chemical vapor deposition (CVD) on Grade 92 (Fe-9Cr-2W) and type 316 stainless steel in isothermal Pb-Li experiments. Specimens of oxide dispersion strengthened (ODS) ferritic steel (14YWT, Fe-14Cr) were exposed in the same CVD reactor using similar conditions. However, the measured mass gains were extremely low compared to other wrought and ODS materials. After aluminizing at 900°C with two Al activities and at 1100°C, characterization showed that 14YWT formed a dense, primarily AlN layer that prevented Al uptake. Since the N content of 14YWT is similar to other FM steels aluminized, this result suggests that the combined O and N contents and the unique microstructure with a fine (~140 nm) grain size and Y-Ti oxide nano-clusters lead to this behavior. If 14YWT cannot be aluminized, another strategy for reducing dissolution in Pb-Li will need to be developed.

PROGRESS AND STATUS

Introduction

A current focus of the U.S.fusion materials program is to address issues associated with the dual coolant Pb-Li (DCLL) blanket concept[1] for a test blanket module (TBM) for ITER and enhanced concepts for a DEMO-type fusion reactor. A DCLL blanket has both He and eutectic Pb-Li coolants and uses reduced activation ferritic-martensitic (FM) steel as the structural material with a SiC/SiC composite flow channel insert (FCI). Thus, recent U.S. compatibility research has examined compatibility issues with Pb-Li.[2-8] Compared to Li,[9] a wider range of materials can be compatible with Pb-Li because of the low activity of Li.[10] In particular, SiC and α-Al_2O_3 readily dissolve in Li, but not in Pb-17Li.[3,4,9,11] However, because of higher Ni and Fe solubilities, Pb-Li readily dissolves many conventional alloys above 500°C. This is not a concern for a DCLL TBM operating at <500°C, however, a DCLL blanket for a commercial reactor would be more attractive with a higher maximum operating temperature, perhaps >600°C if ODS FM steels[12,13] were used. Even at 550°C, a recent study of Eurofer 97 (Fe-Cr-W) showed a very high dissolution rate in flowing Pb-Li.[14] Therefore, preliminary Pb-Li compatibility capsule experiments are being conducted at 500°-800°C in order to investigate several concepts before flowing Pb-Li compatibility tests are conducted. Prior work has shown that alloys that contain Al or have an Al-rich coating show dramatically lower mass losses in 1kh Pb-Li capsule tests than alloys without Al, Figure 1. However, it has not been possible to aluminize the ODS Fe-14Cr alloy (14YWT) and those CVD results and characterization of the 14YWT specimens after exposure in the CVD reactor are presented here.

Experimental Procedure

The composition of the aluminized alloys is given in Table 1. The results for 14YWT and 754 are preliminary values from other heats and need to be measured for the particular batch of material used in these experiments (SM10) which also had a very fine grain size (~140nm). Composition is being

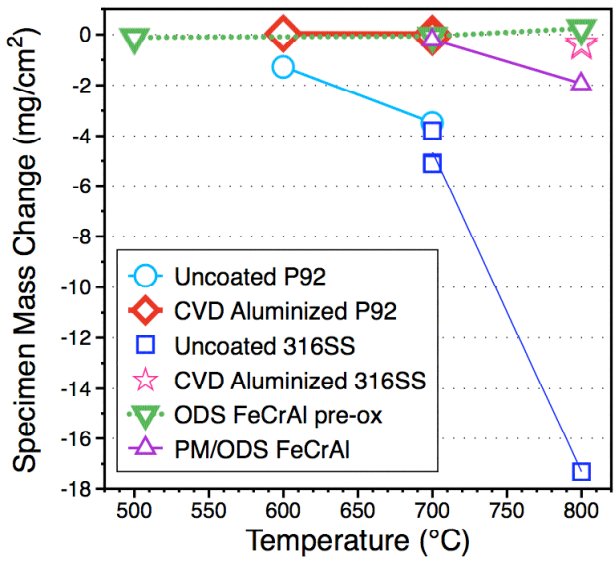

Figure 1. Specimen mass loss as a function of exposure temperature in Pb-Li for 1kh in Mo capsules. Alumina-forming alloys or coatings have much lower mass losses than conventional Fe-base alloys.[4-6]

measured for the new Fe~14Cr ODS alloy, 401 (designated ODM401 by its manufacturer Dour Metal sro). Prior to aluminizing, specimens were polished to a 0.3 μm alumina finish and cleaned ultrasonically in acetone and alcohol. Aluminizing was performed in a laboratory-scale CVD reactor consisting of an inductively heated alumina tube with flowing H_2 carrying the $AlCl_x$ vapor. The reactor has been described in detail elsewhere.[15,16] Typically, four specimens were hung from two alumina rods and are designated

Table 1. Alloy chemical compositions (atomic% or ppma) determined by inductively coupled plasma analysis and combustion analysis.

Material	Fe	Ni	Cr	Al	O	C	N	S	Other
14YWT	84.5		14.0	0.04	3940	2440	**1540**	52	0.2W,0.14Y 0.22Ti,0.16Si
Gr.91 (9Cr-1Mo)	87.8	0.1	9.9		90	2380	**1900**	14	0.6Mo,0.3V, 0.5Mn,0.4Si,
P92 (9Cr-2W)	87.2	0.1	9.9	0.02	80	5120	**2330**	87	0.55W, 0.46Mn 0.30Mo,0.32Si
754	0.4	74.9	21.4	0.7	15100	2300	n.d.	20	0.53Ti,0.36Y
740	2.0	46.2	25.3	1.7	60	3650	460	<	19.3Co,2,3Ti,1.2Nb 0.9Si,0.3Mn,0.3Mo
X	18.7	46.5	24.8	0.2	33	3260	1680	<	5.8Mo,1.8Co 0.2W,0.7Mn,0.6Si
N5	0.1	64.8	7.8	13.9	52	2490	<	7	7.3Co,2.1Ta,1.6W 1Re,0.9Mo,0.05Hf,0.003Y

< indicates below the detectability limit of <0.01% or <0.001% for interstitials

front or back with relation to the flowing gas stream. The front specimens typically had 10-30% higher mass gain. An Al-60wt.%Cr powder was added to the reactor to increase the Al activity for some runs at 900°C, but not at 1100°C. The specimen mass change was measured before and after aluminizing with an accuracy of ±0.01 mg/cm^2. A summary of the conditions and mass change data for the ODS specimens is given in Table 2. After aluminizing, the specimens were examined by x-ray diffraction (XRD), x-ray photoelectron spectroscopy (XPS) and scanning electron microscopy (SEM) equipped with energy dispersive x-ray (EDX) analysis. For cross-sectioning, a focused ion beam (FIB) was used.

Results and Discussion

The mass gain data for the two CVD aluminizing temperatures are shown in Figures 2 and 3 and the data for the ODS alloys are summarized in Table 2. (The comparison mass gain data are from a variety of different programs that have made coatings for fossil energy applications in the same CVD reactor.[17-19]) At 900°C, the mass gain for the 14YWT material was much lower than other FM steels (Grades 91 and 92) at 900°C and even lower than the ODS and wrought austenitic Ni-base alloys (754 and X) which have slower Al diffusivity than the ferritic alloys. The mass gain was slightly higher for the 14YWT specimens when Al-Cr powder was added to the reactor but orders of magnitude lower than the all the comparison materials. At 1100°C, the 14YWT specimen lost mass while the Ni-base alloys all gained mass, forming a NiAl coating. (No other Fe-base alloys were aluminized as the coating would be very thick (>250μm).[16] Only one commercial ODS FeCr alloy (401) was recently made available for comparison to 14YWT, therefore, an ODS NiCr alloy, 754 (designated MA754 by manufacturer Special Metals), was included in two runs adjacent to the 14YWT specimen for a direct comparison. At both temperatures, the 754 specimen mass gain was significantly higher than the 14YWT specimen, gaining more mass than the comparable Ni-base alloys at 900° and 1100°C.

In order to determine why the 14YWT specimen did not gain mass during aluminizing, the characterization compared the 14YWT and 754 specimens as both are dispersion strengthened alloys. Figures 4 and 5 show the surface morphology of both materials after aluminizing. For Ni-base alloys, the morphology of 754 after 6h at 1100°C, Figure 5c, is a typical aluminized morphology with NiAl grain boundaries clearly evident and slight ridges forming on most boundaries.[15,17] At 900°C, the aluminide grains appear to be finer on 754 with similar grain boundary ridges, Figure 4c. In contrast, the surface of 14YWT at both temperatures was much different with fewer distinctive features, Figures 4a and 5a. Higher magnification images of the 14YWT surface are shown in Figures 4b and 5b that suggest a much finer grained surface layer, nothing like an aluminide structure.

Table 2. Mass change of ODS specimens in CVD aluminizing for 6h in laboratory reactor.

Specimen	Temperature	Powder	Location	Mass Change (mg/cm^2)
14YWT	1100°C	No	Front	-0.61
	900°C	Al/Cr	Front	0.05
				0.06
				0.15
		No	Back	0.02
754 (NiCr)	1100°C	No	Front	8.02
	900°C	Al/Cr	Back	1.54
401 (FeCr)	900°C	No	Back	1.30

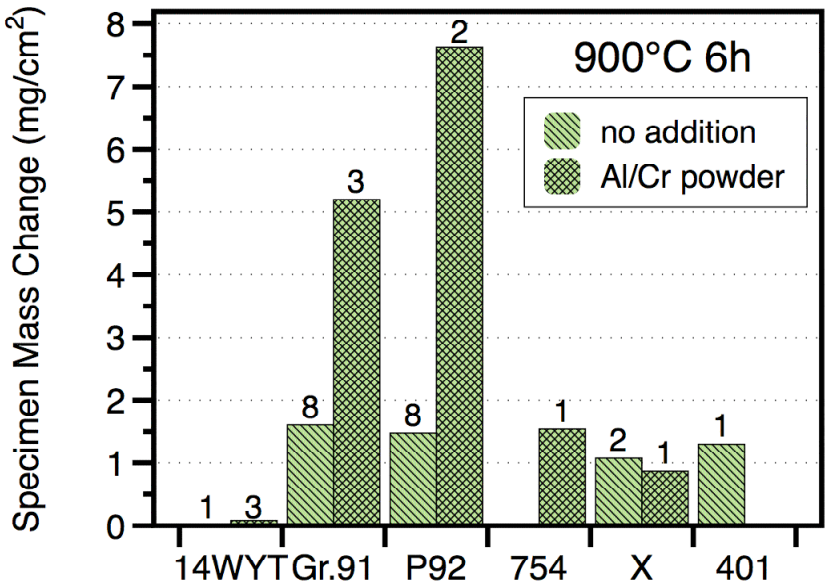

Figure 2. Average specimen mass change after 6h at 900°C in a laboratory-scale CVD reactor with and without Al-Cr powder to raise the Al activity and increase the Al uptake. The numbers mark the number of specimens exposed.

Based on the low mass change for 14YWT, a thin reaction product was expected that could be studied by a surface analytical technique such as XPS. Figure 6 shows sputter depth profiles for 14YWT after CVD exposures at 900° and 1100°C. The sputter depth is estimated based on the sputter crater depth. At 900°C, the surface is rich in Al, O and N with the O signal falling off faster than the N signal. Based on

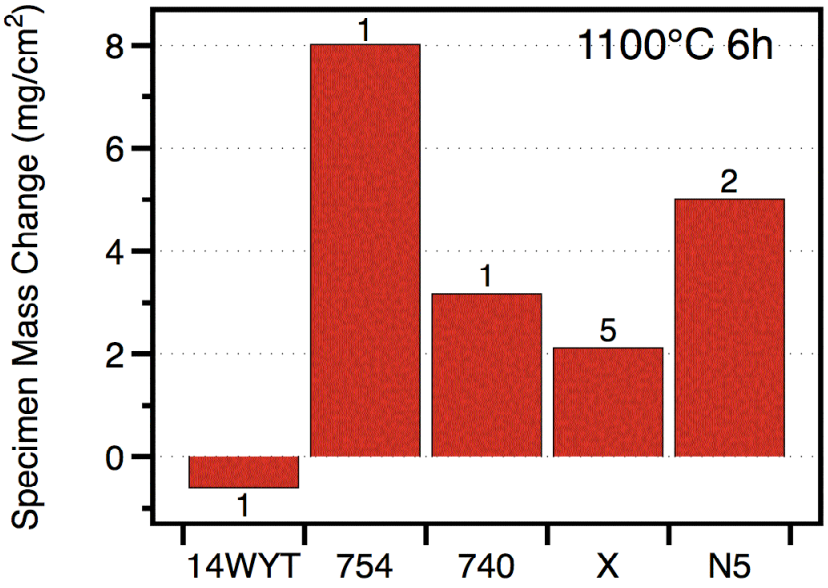

Figure 3. Average specimen mass change after 6h at 1100°C in a laboratory-scale CVD reactor. The numbers mark the number of specimens exposed.

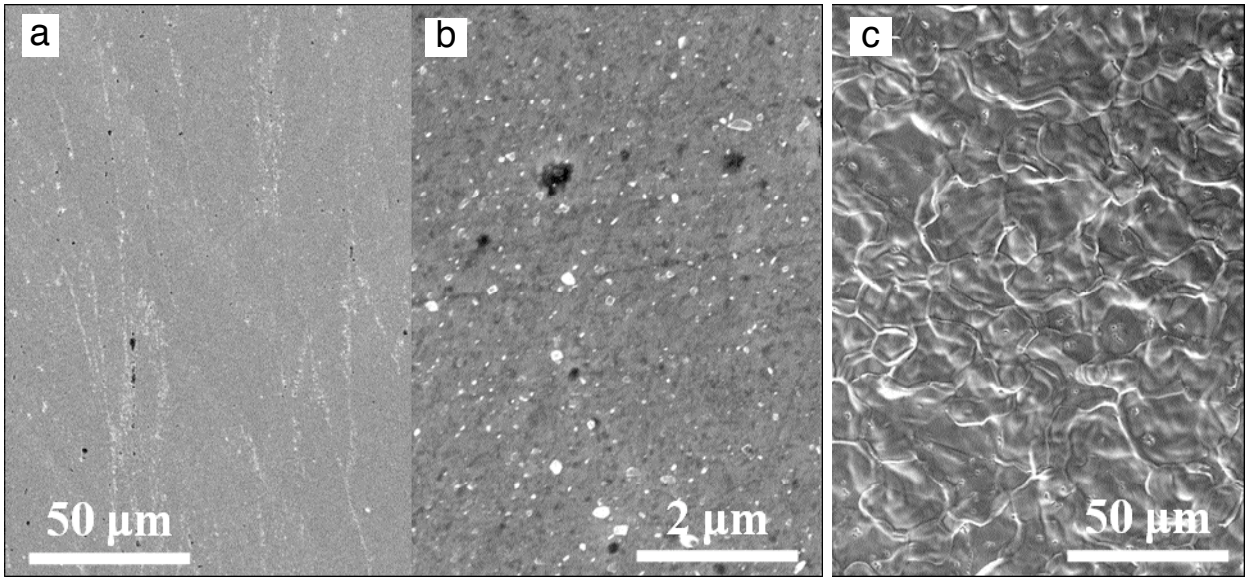

Figure 4. SEM plan view images of the specimen surface after aluminizing for 6h at 900°C with Al-Cr powder (a,b) 14YWT and (c) 754.

the cross-over of the Fe and Al signals, this outer Al-rich oxy-nitride layer appears to be less than 100 nm in thickness. The Al signal drops to background levels by 175 nm. Typically, FM steels aluminized under these conditions would show ~32-36 at.%Al at the surface with an Al profile extending 100 μm into the substrate. These deep Al profiles were observed with coating mass gains of 5-7 mg/cm^2, Figure 2. At 1100°C, the reaction product on 14YWT was much thicker but appeared to be more concentrated in N than at 900°C, Figure 6b. Again based on the Al-Fe signal cross-over, the surface reaction product appeared

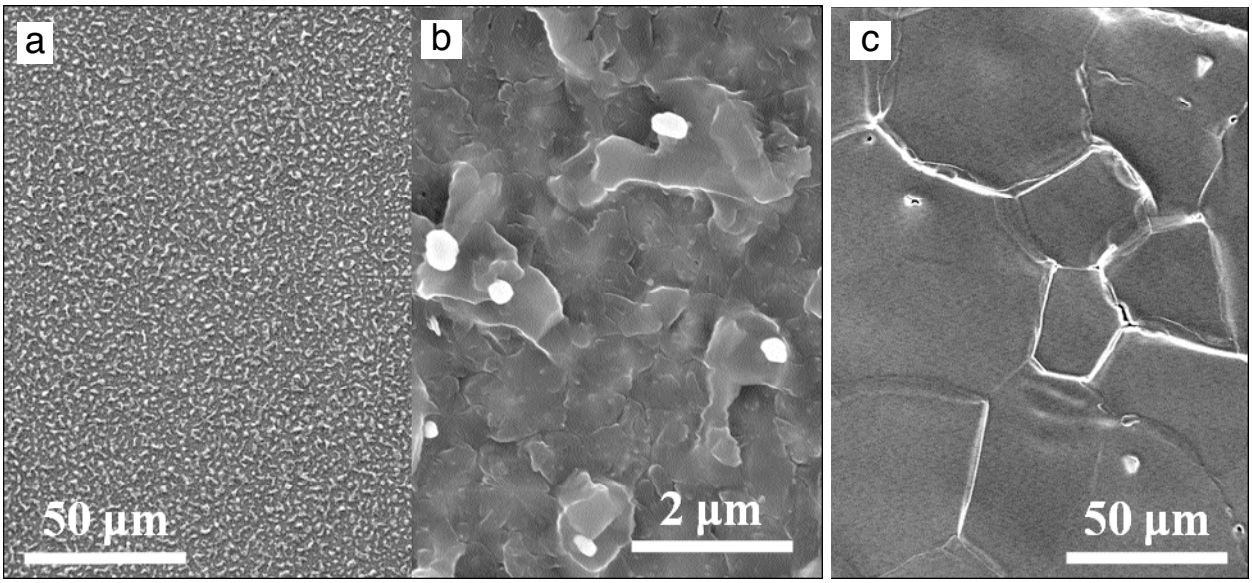

Figure 5. SEM plan view images of the specimen surface after aluminizing for 6h at 1100°C (a,b) 14YWT and (c) 754.

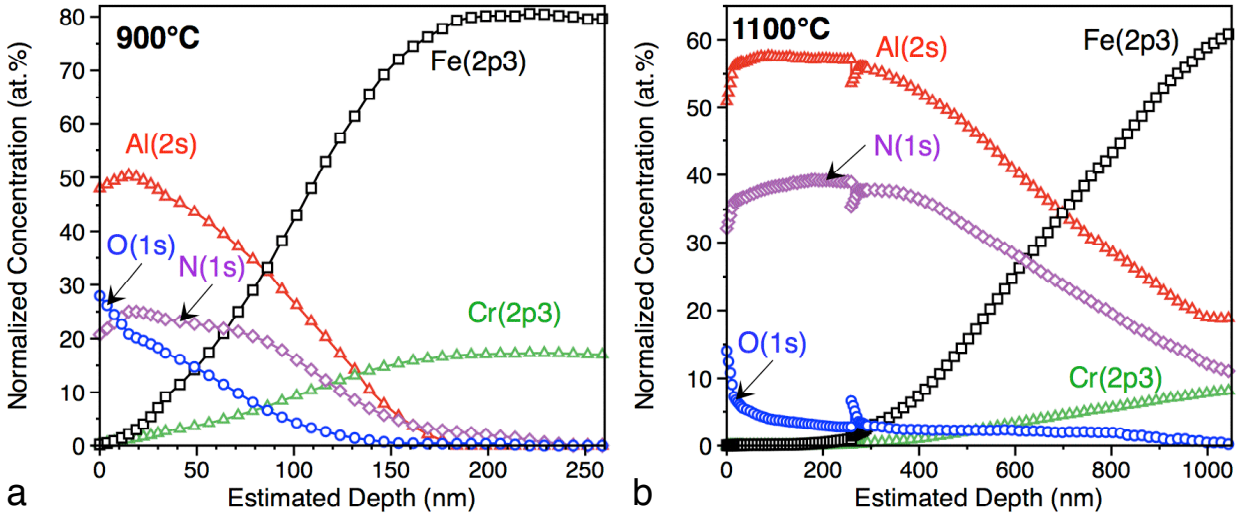

Figure 6. XPS sputter depth profiles of 14YWT after aluminizing (a) 900°C with powder and (b) 1100°C. The outer surface is rich in Al, O and N in both cases. In (b), the signal change at ~250μm is where the sputtering was stopped and restarted in the same location.

to be ~700 nm thick. The composition change at ~250 μm depth is where the XPS sputtering was stopped and then restarted at the same location. The formation of this surface AlN layer on 14YWT is not consistent with the mass loss observed after exposure, Table 2. One possibility is that some Fe was removed from the surface by the Cl in the environment, as suggested by Kung and Rapp.[20] The surface of the aluminized 754 specimens also was sputtered by XPS for comparison. Figure 7 shows that after both CVD temperatures, a ~10 nm oxide layer was detected on the surface of the aluminide layer with

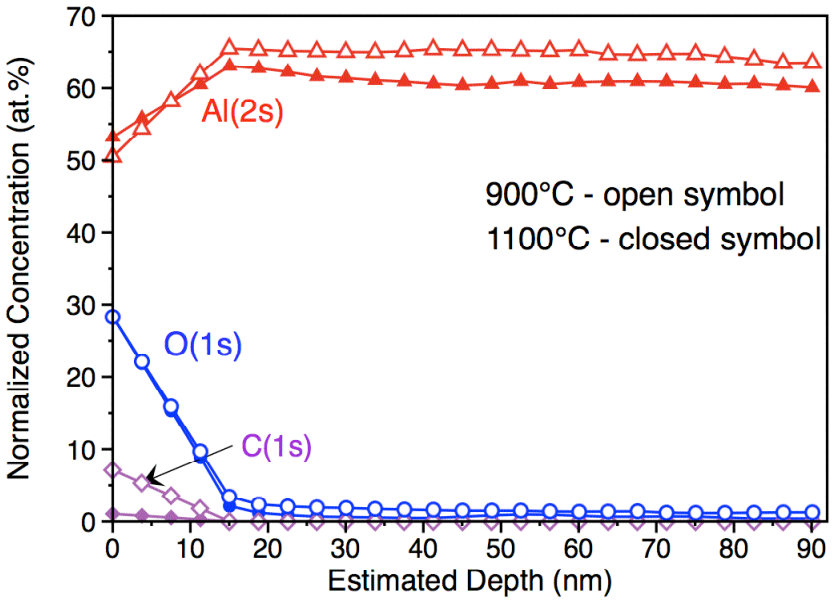

Figure 7. XPS sputter depth profiles of 754 after aluminizing, the 900°C data are shown with open symbols and the 1100°C data with closed symbols.

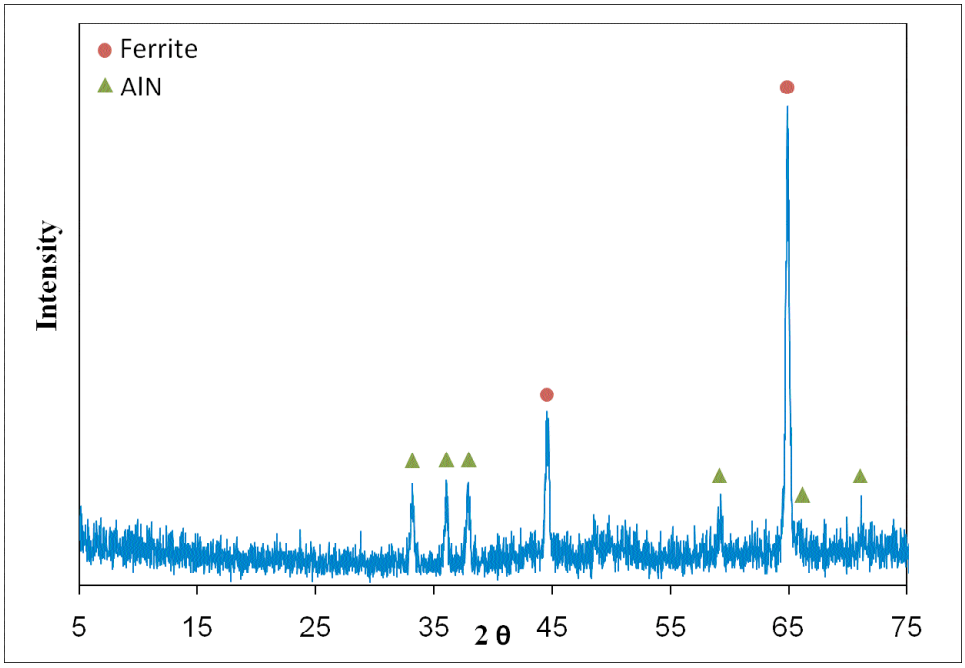

Figure 8. XRD spectra from 14YWT after CVD exposure at 1100°C.

some C present. This is more typical of the native oxide expected on a CVD aluminized substrate.

The reaction layer on 14YWT after the 1100°C CVD exposure was further characterized by XRD and FIB sectioning. In the XRD spectra, the ferritic matrix and the AlN peaks are labeled, confirming the presence of a nitride layer, Figure 8. Figure 9 shows a cross-section of the reaction product prepared by FIB sectioning. A W coating was deposited on the surface to protect the reaction product during sectioning by the ion beam. In this region, the reaction product appears to be continuous and at least 250 nm thick, less than that suggested by the XPS sputtering profile. However, quantifying the sputtering rate can be difficult and may have over estimated the AlN thickness. Also, the layer thickness may not be uniform on the specimen.

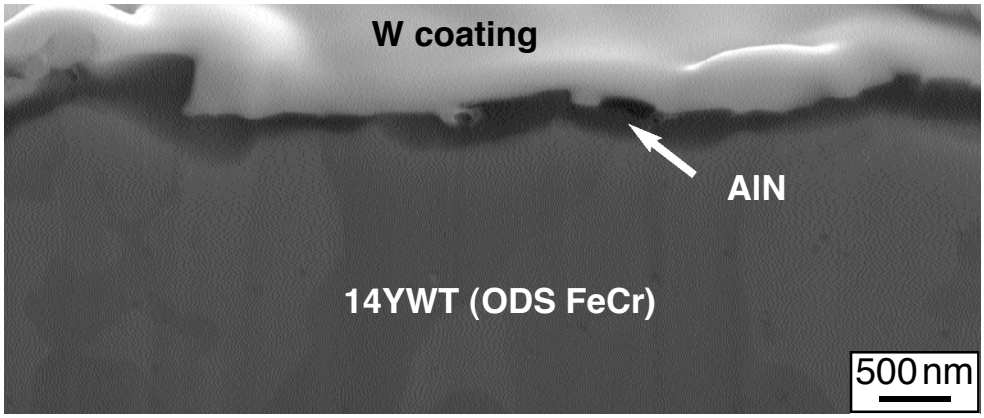

Figure 9. SEM image of FIB cut cross-section of 14YWT after aluminizing at 1100°C. The surface was coated with a layer of W for protection.

The N content in 14YWT is the likely source of N to form the AlN layer as no nitride layer was observed on aluminized 754 or on other FM specimens. Table 1 shows that the nominal N content in 14YWT is not expected to be higher than levels in other FM steels. With these N levels, FM steels routinely form acicular AlN precipitates in the coating which coarsen with exposure time,[16,19,21] but there is no indication of a continuous surface layer as was observed for 14YWT specimens. The source of the AlN precipitates in aluminized FM steels was clearly shown to be the N in the alloy by low-N model alloy experiments.[22] Nickel-base alloy X was chosen for comparison because it also contains a high N content which does not inhibit aluminizing. The reason 14YWT behaves differently than FM steels in aluminizing may be due to the combination of N and O in the alloy. Of course, all ODS alloys have high N and O contents compared to conventional alloys due to the nature of the powder metallurgy process used for fabrication. Neither 754 (NiCr) nor 401 (FeCr) showed a similar problem as 14YWT. One reported unique aspect of 14YWT is the high density of Y-Ti oxide “nano-clusters”. If the O distribution is different in 14YWT than other ODS alloys, the fine dispersion may more readily allow the rapid formation of an Al-rich oxide layer in the CVD environment that could inhibit Al uptake in this alloy. Both XPS profiles suggest a high O concentration at the surface. After the Al-rich oxide layer forms, the N content in the alloy could then continue to react with Al forming the underlying AlN layer at a rate dependent on the temperature.

Regardless of the mechanism, a different strategy may be needed for protecting 14YWT from dissolution in Pb-Li. Now that it is apparent that 14YWT will not be coated by the CVD process used for other materials on this project, uncoated 14YWT specimens are being prepared for Pb-Li capsule exposures.

References

[1] M. Abdou, D. Sze, C. Wong, M. Sawan, A. Ying, N. B. Morley and S. Malang, Fus. Sci. Tech., 47 (2005) 475.
[2] B. A. Pint J. L. Moser and P. F. Tortorelli, Fus. Eng. Des. 81 (2006) 901.
[3] B. A. Pint, J. L. Moser and P. F. Tortorelli, J. Nucl. Mater. 367-370 (2007) 1150.
[4] B. A. Pint, Fus. Sci. Tech. 52 (2007) 829.
[5] B. A. Pint and K. L. More, J. Nucl. Mater. 376 (2008) 108.
[6] B. A. Pint, Mater. Sci. Forum, 595-598 (2008) 549.
[7] B. A. Pint, J. Nucl. Mater., in press.
[8] B. A. Pint and K. A. Unocic, DOE/ER-0313/47 (2009) 82.
[9] J. E. Battles, Intern. Mater. Rev. 34 (1989) 1.
[10] P. Hubberstey, J. Nucl. Mater. 247 (1997) 208.
[11] T. Yoneoka, S. Tanaka and T. Terai, Mater. Trans. 42 (2001) 1019.
[12] S. Ukai and M. Fujiwara, J. Nucl. Mater. 307 (2002) 749.
[13] R. L. Klueh, J. P Shingledecker, R. W. Swindeman, D. T. Hoelzer, J. Nucl. Mater. 341 (2005) 103.
[14] J. Konys, W. Krauss, J. Novotny, H. Steiner, Z. Voss and O. Wedemeyer, J. Nucl. Mater. 386-88 (2009) 678.
[15] Y. Zhang, W. Y. Lee, J. A. Haynes, I. G. Wright, B. A. Pint, K. M. Cooley and P. K. Liaw, Met. Trans. 30A (1999) 2679.
[16] Y. Zhang, B. A. Pint, K. M. Cooley and J. A. Haynes, Surf. Coat. Tech. 202 (2008) 3839.
[17] J. A. Haynes, B. A. Pint, K. L. More, Y. Zhang, and I. G. Wright, Oxid. Met. 58 (2002) 513.
[18] B. A. Pint, J. A. Haynes and T. M. Besmann, Surf. Coat. Technol., 204 (2010) 3287.
[19] B. A. Pint and Y. Zhang, Mater. Corr., in press.
[20] S. C. Kung and R. A. Rapp, Oxid. Met., 32 (1989) 89.
[21] A. Agüero, K. Spiradek, S. Hoefinger, M. Gutierrez and R. Muelas, Mater. Sci. Forum, 595-598 (2008) 251.
[22] Y. Zhang, B. A. Pint, K. M. Cooley and J. A. Haynes, Surf. Coat. Technol., 200 (2005) 1231.
[23] M. K. Miller, E. A. Kenik, K. F. Russell, L. Heatherly, D. T. Hoelzer and P. J. Maziasz, Mater. Sci. Eng. A, 353 (2003) 140-145.